Dynamical Resolution of Redundancy for Robot Manipulators

A. Ghosal
Department of Mechanical Engineering,
Indian Institute of Science,
Bangalore-560012, India

S. Desa
Department of Mechanical Engineering,
Carnegie-Mellon University,
Pittsburgh, PA 15213

A large class of work in the robot manipulator literature deals with the kinematical resolution of redundancy based on the pseudo-inverse of the manipulator Jacobian. In this paper an alternative dynamical approach to redundancy resolution is developed which utilizes the mapping between the actuator torques and the acceleration of the end-effector, at a given dynamic state of the manipulator. The potential advantages of the approach are discussed and an example of a planar 3R manipulator following a circular end-effector trajectory is used to illustrate the proposed approach as well as to compare it with the more well-known approach based on the pseudo-inverse.

1 Introduction

The task or primary function of a vast majority of manipulators is to cause the end-effector to follow a desired trajectory. If the number of degrees of freedom of the manipulator are in excess of those required by the task, then the manipulator is referred to as a redundant manipulator. The number of degrees of redundancy of a manipulator is defined as the number of excess degrees of freedom which the manipulator possesses. A redundant manipulator offers the possibility, at the cost of increased complexity, of exploiting its degrees of redundancy in order to perform useful secondary functions, for example, avoidance of obstacles or singularities [1]. (Actual redundant manipulator systems for various applications are described in [2-5].) A direct consequence of redundancy is that, corresponding to a given end-effector trajectory, there are an infinite number of possible manipulator configurations. Therefore a central problem in task planning or motion planning for redundant manipulators is the choice of a suitable configuration from the set of infinite possible configurations. This problem, referred to in the literature as the resolution of redundancy, is the central theme of the present paper.

One popular set of methods for the resolution of redundancy revolves around the use of the pseudo-inverse of the manipulator Jacobian [6-18]. Most of the pseudo-inverse methods, with the exception of [15-16] and [17-18], are primarily kinematical in nature. Furthermore the pseudo-inverse methods do not allow the user to exploit the actual number of degrees of redundancy. In this paper we propose an alternative method of resolving redundancy which has the following features:

(*a*) it is based on the mapping between the actuator torques and the acceleration of the end-effector, at a given dynamic state of the manipulator,

(*b*) it treats the actuator torques as the inputs or primary variables which can be manipulated to achieve desirable performance objectives,

(*c*) it allows the user to exploit all the available number of degrees of redundancy.

(The meaning of the last statement is clarified in Section 2.)

The approach to redundancy resolution presented in this paper is particularly appealing since the primary variables used to resolve redundancy, the actuator torques, are the natural set of inputs which control the motion of the manipulator. The proposed approach is the dynamical counterpart of a differential-geometric approach to the kinematical resolution of redundancy, reported in [19, 20], which was based on altering local kinematic properties.

1.1 Outline of the Contents. In the rest of this section we more formally define the redundancy resolution problem and then review the pseudo-inverse method of redundancy resolution. To set the stage for our approach to dynamical redundancy resolution, we first present the dynamic mapping between the joint-torques and the end-effector acceleration for nonredundant manipulators (Section 2). The mapping between the actuator torques and end-effector acceleration for redundant manipulators follows in a relatively straightforward manner from the results of Section 2. The use of this mapping to dynamically resolve redundancy is then discussed in Section 3, followed by a description of the numerical algorithm for planning trajectories based on our method. In Section 4, we use the example of a planar 3R manipulator following a prescribed circular end-effector trajectory, to demonstrate the application of the proposed approach. The paper concludes with a critical discussion of our approach to the dynamical resolution of redundancy.

1.2 Statement of the Redundancy Resolution Problem. Consider the motion in three-dimensional space of the end-effector of an m degree-of-freedom spatial manipulator

Contributed by the Mechanisms Committee and presented at the Design Technical Conference, Chicago, IL, Sept. 16-19, 1990, of THE AMERICAN SOCIETY OF MECHANICAL ENGINEERS. Manuscript received March 1990; revised August 1991. Associate Technical Editor: J. M. McCarthy.

n a reference-frame R. Let $\Theta = (\theta_1, \theta_2, \ldots \theta_m)$ be a vector of he joint-variables and let $\mathbf{E}$ be a vector of the n ($n \leq 6$) coordinates which specify the position and orientation of the end-effector in the reference-frame R. Let Θ also represent the n-dimensional "joint-space" of the manipulator and let $\mathbf{E}$ also represent the n-dimensional "task-space" of the manipulator. A point in the joint space then represents a configuration of the manipulator and a point in the task-space $\mathbf{E}$ represents the position and orientation of the end-effector. Let Ψ denote the vector of n functions which prescribe the position and orientation of the end-effector for a given configuration of the manipulator. We can then regard Ψ: $\Theta - \mathbf{E}$ as the mapping between a point in the m-dimensional "joint-space" Θ and the corresponding point in the n-dimensional "task-space" $\mathbf{E}$.

For the most general case of spatial motion of the end-effector in $\mathbf{R}^3$, $n = 6$. If the number of degrees of freedom m of the manipulator is greater than n, then the manipulator is said to possess $(m-n)$ degrees of redundancy. A manipulator with $(m-n)>0$ degrees of redundancy is often referred to simply as a "redundant manipulator," with $(m-n)$ degrees of redundancy.

For a nonredundant manipulator, corresponding to a vector in the task space (i.e., a given end-effector position and orientation) there are, in general, only a finite (unique) set of possible joint-space solutions, i.e., the mapping Ψ is invertible. For a redundant manipulator with $(m-n)$ degrees of redundancy, corresponding to a vector in the task space there are $\infty^{(m-n)}$ joint-space solutions, i.e., the mapping Ψ is noninvertible. This fact leads directly to the problem which has been referred to in the literature as the resolution of redundancy, viz., the problem of obtaining a joint-space solution $(\theta_1, \ldots, \theta_m)$ for a given task-space vector $\mathbf{E}$ from the infinity of possible joint-space solutions. It should be emphasized that in the resolution of redundancy one would like to obtain a solution which is not only feasible but also meets some desirable objective.

1.3 Review of Existing Redundancy Resolution Schemes. In general, the problem of obtaining a unique $(\theta_1, \ldots, \theta_m)$ for a given task space vector is complex owing to the fact that the functions defining the mapping Ψ are typically nonlinear. Instead most researchers resolve redundancy at the level of velocity or at the level of joint acceleration by using the Moore-Penrose generalized inverse, also called the pseudo-inverse [21], and then determine $(\theta_1, \ldots, \theta_m)$ by integration. In the context of the present work, it is useful to review the psuedo-inverse based schemes for the resolution of the redundancy at the level of joint acceleration.

Let $\dot{\Theta}$ denote $(\dot{\theta}_1, \ldots, \dot{\theta}_m)^T$. We can express the end-effector velocity $\dot{\mathbf{E}}$ as

$$\dot{\mathbf{E}} = J\dot{\Theta} = \sum_{i=1}^{m} \Psi_i \dot{\theta}_i, \tag{1}$$

where $\mathbf{J}$ is the $(n \times m)$ Jacobian matrix whose ith column Ψ_i is $\partial\Psi/\partial\theta_i$. The acceleration $\ddot{\mathbf{E}}$ can be written as

$$\ddot{\mathbf{E}} = \mathbf{J}\ddot{\Theta} + \dot{\mathbf{J}}\dot{\Theta} = \sum_{i=1}^{m} \Psi_i \ddot{\theta}_i + \sum_{i=1}^{m}\sum_{j=1}^{m} \Psi_{ij}\dot{\theta}_i\dot{\theta}_j, \tag{2}$$

where $\ddot{\Theta}$ is $(\ddot{\theta}_1, \ldots, \ddot{\theta}_m)^T$, $\dot{\mathbf{J}}$ is the derivative of the Jacobian matrix, and Ψ_{ij} is $\partial^2\Psi/\partial\theta_i\partial\theta_j$ ($i = 1, 2, \ldots m$), ($j = 1, 2, \ldots m$).

The dynamic equations of motion of a manipulator can be written as

$$\Gamma = \mathbf{M}(\Theta)\ddot{\Theta} + \mathbf{C}(\Theta, \dot{\Theta}) + \mathbf{g}(\Theta), \tag{3}$$

where Γ is the $(m \times 1)$ vector of actuator torques, $\mathbf{M}(\Theta)$ is the $(m \times m)$ mass matrix, $\mathbf{C}(\Theta, \dot{\Theta})$ is the $(m \times 1)$ vector of Coriolis, centrifugal, and friction terms and $\mathbf{g}(\Theta)$ is the $(m \times 1)$ vector of gravity terms.

Khatib [15, 16] used the pseudo-inverse of $\mathbf{J}$ at the joint acceleration level for the resolution of redundancy and for control. He used the inertia-weighted pseudo-inverse $\mathbf{J}_{\bar{M}}^{\#}$, and obtained $\ddot{\Theta}$ as follows:

$$\ddot{\Theta} = \mathbf{J}_{\bar{M}}^{\#}(\ddot{\mathbf{E}} - \dot{\mathbf{J}}\dot{\Theta}). \tag{4}$$

In [17, 18], Hollerbach and Suh used the pseudo-inverse of $\mathbf{J}$ together with a null-space term to minimize $\|\Gamma - (1/2)(\alpha+\beta)\|^2$, where α and β are the $(m \times 1)$ vectors of upper and lower torque limits at the joints, respectively. In their approach $\ddot{\Theta}$ is obtained as

$$\ddot{\Theta} = \mathbf{J}^{+}(\ddot{\mathbf{E}} - \dot{\mathbf{J}}\dot{\Theta}) + (\mathbf{I} - \mathbf{J}^{+}\mathbf{J})\ddot{\mathbf{F}}, \tag{5}$$

where $(\mathbf{I} - \mathbf{J}^{+}\mathbf{J})\ddot{\mathbf{F}}$ is the null-space vector, and $\ddot{\mathbf{F}}$ was given by

$$\ddot{\mathbf{F}} = (1/2)[\mathbf{M}(\mathbf{I} - \mathbf{J}^{+}\mathbf{J})]^{+}(\alpha' + \beta'). \tag{6}$$

In the above equation, $\alpha' = \alpha - \Gamma'$, $\beta' = \beta - \Gamma'$, and

$$\Gamma' = \mathbf{M}\mathbf{J}^{+}(\ddot{\mathbf{E}} - \dot{\mathbf{J}}\dot{\Theta}) + \mathbf{C}(\Theta, \dot{\Theta}) + \mathbf{g}(\Theta). \tag{7}$$

The pseudo-inverse method of redundancy resolution can be viewed as an attempt to solve the redundant manipulator problem in a manner suggested by the solution of the corresponding nonredundant manipulator problem. In this regard the method does not exploit the actual number of degrees of redundancy; for example, it cannot differentiate ten degrees of redundancy (say) from one degree of redundancy. Therefore the analyst cannot clearly see the effect of increasing the degrees of redundancy in a given problem. Furthermore, it is not possible to satisfy more than one performance criteria even in the case where we have more than 1 redundant degree of freedom. In contrast to the pseudo-inverse method, we will present a straightforward approach to the (dynamical) resolution of redundancy which is based on the kinematical and dynamical equations of the manipulator and which allows the analyst to make use of all the available degrees of redundancy. In order to develop a better understanding of the proposed approach, we first discuss the dynamics of nonredundant manipulators.

2 Dynamics of Nonredundant Motions

In this section we review the relationship between the actuator torques and the end-effector acceleration for a nonredundant manipulator. This review will also facilitate the differentiation of the nonredundant case (discussed in Section 3) from the redundant case. Let $\mathbf{p}(x, y, z)$ be the Cartesian coordinates in $\mathbf{R}^3$ of a reference point on the end-effector of a three degrees-of-freedom manipulator. The trajectories of this reference point lie in a bounded "solid" region in $\mathbf{R}^3$. The invertible mapping between manipulator configuration $(\theta_1, \theta_2, \theta_3)$ and end-effector position can be written as

$$(x, y, z)^T = \Psi(\theta_1, \theta_2, \theta_3). \tag{8}$$

The velocity, $\mathbf{v}$, at any generic position $\mathbf{p}$ in $\mathbf{R}^3$ [the image of a generic configuration $(\theta_1, \theta_2, \theta_3)$] is given by

$$\mathbf{v} = \mathbf{J}(\Theta)\dot{\Theta} = \Psi_1\dot{\theta}_1 + \Psi_2\dot{\theta}_2 + \Psi_3\dot{\theta}_3, \tag{9}$$

where $\mathbf{J}(\Theta)$ is the (3×3) invertible Jacobian matrix corresponding to the position $\mathbf{p}$ and $\Psi_i = (\partial\Psi/\partial\theta_i)$, $(i = 1, 2, 3)$, is the ith column of $\mathbf{J}(\Theta)$.

The acceleration of the reference-point can be written as

$$\mathbf{a} = \mathbf{J}(\Theta)\ddot{\Theta} + \dot{\mathbf{J}}(\Theta)\dot{\Theta} = \sum_{i=1}^{3} \Psi_i\ddot{\theta}_i + \sum_{i=1}^{3}\sum_{j=1}^{3} \Psi_{ij}\dot{\theta}_i\dot{\theta}_j, \tag{10}$$

where $\dot{\mathbf{J}}(\Theta)$ is the derivative of the Jacobian (with respect to time) evaluated at the position of interest and $\Psi_{ij} = \partial^2\Psi/\partial\theta_i\partial\theta_j$. The equations of motion for a three-degree-of-freedom mechanism can be symbolically written as

$$\Gamma = \mathbf{M}(\Theta)\ddot{\Theta} + \mathbf{C}(\Theta, \dot{\Theta}) + \mathbf{g}(\Theta), \tag{11}$$

where Γ is $(\tau_1, \tau_2, \tau_3)^T$, the (3×1) vector of the actuator torques applied at the joints, $\mathbf{M}(\Theta)$ is the (3×3) symmetric positive definite mass matrix, $\mathbf{C}(\Theta, \dot{\Theta})$ is the (3×1) vector of

the Coriolis, centripetal, and friction terms, and $\mathbf{g}(\boldsymbol{\Theta})$ is the (3 × 1) vector of gravity terms. Since $\mathbf{M}(\boldsymbol{\Theta})$ is always invertible, we can combine (10) and (11) to obtain the following expression for acceleration:

$$\mathbf{a} = \mathbf{J}(\boldsymbol{\Theta})\mathbf{M}(\boldsymbol{\Theta})^{-1}\,[\boldsymbol{\Gamma} - \mathbf{C}(\boldsymbol{\Theta}, \dot{\boldsymbol{\Theta}}) - \mathbf{g}(\boldsymbol{\Theta})] + \dot{\mathbf{J}}\dot{\boldsymbol{\Theta}}. \tag{12}$$

Finally, denoting the three columns of $\mathbf{J}(\boldsymbol{\Theta})\mathbf{M}(\boldsymbol{\Theta})^{-1}$ by $\boldsymbol{\mu}_i$, $(i = 1,2,3)$, and defining,

$$\boldsymbol{\eta}(\boldsymbol{\Theta}, \dot{\boldsymbol{\Theta}}) = \dot{\mathbf{J}}\dot{\boldsymbol{\Theta}} - \mathbf{J}\mathbf{M}^{-1}[\mathbf{C}(\boldsymbol{\Theta}, \dot{\boldsymbol{\Theta}}) + \mathbf{g}(\boldsymbol{\Theta})], \tag{13}$$

we can express the end-effector acceleration in the following useful form:

$$\mathbf{a} = \boldsymbol{\mu}_1\tau_1 + \boldsymbol{\mu}_2\tau_2 + \boldsymbol{\mu}_3\tau_3 + \boldsymbol{\eta}(\boldsymbol{\Theta}, \dot{\boldsymbol{\Theta}}) \tag{14}$$

where τ_i, $(i = 1, 2, 3)$, is the actuator torque applied at the ith joint. Equation (14) is fundamental to our approach for dynamical redundancy resolution. We can make the following observations from Eq. (14):

(1) The vectors $\boldsymbol{\mu}_i$, $(i = 1, 2, 3,)$ are functions only of $\boldsymbol{\Theta}$, and, at a given position $\mathbf{p}$, the map ξ_{Γ}:$\boldsymbol{\Gamma} - \mathbf{a}$ is linear. The map $\xi_{\dot{\Theta}}$:$\dot{\boldsymbol{\Theta}} - \mathbf{a}$ (at a given position) is quadratic. The properties of this mapping are extensively discussed in [22]. At a given state, i.e., known $(\boldsymbol{\Theta}, \dot{\boldsymbol{\Theta}})$, the nonlinear term, $\boldsymbol{\eta}(\boldsymbol{\Theta}, \dot{\boldsymbol{\Theta}})$, is a known constant vector.

(2) At a given state, the direction and the magnitude of the acceleration vector changes with respect to τ_i, $(i = 1, 2, 3)$. Without any constraint on the torques, the acceleration vectors fill up all of $\mathbf{R}^3$. With a typical constraint of the form $\tau_{i,l} \le \tau_i \le \tau_{i,u}$, $(i = 1, 2, 3)$, where $\tau_{i,l}$ and $\tau_{i,u}$ are, respectively, the lower and upper bounds on the ith actuator torque, the set of all allowable acceleration vectors form a parallelopiped as a consequence of the linear mapping between $\boldsymbol{\Gamma}$ and $\mathbf{a}$ [22].

(3) In the case of a nonredundant manipulator, for a given end-effector acceleration $\mathbf{a}$ and a given dynamic state $(\boldsymbol{\Theta}, \dot{\boldsymbol{\Theta}})$ of the manipulator, the actuator torques are uniquely determined from (14).

3 Dynamical Resolution of Redundancy

In this section we describe the dynamical approach to redundancy resolution, demonstrate its application and finally present an algorithm for the implementation of the approach. In contrast to the nonredundant manipulator, for a given end-effector acceleration $\mathbf{a}$ and a given dynamic state $(\boldsymbol{\Theta}, \dot{\boldsymbol{\Theta}})$ of the manipulator, there are an infinite number of feasible combinations of actuator torques. This fact will provide the basis for our dynamical approach to exploiting redundancy.

3.1 Approach. In the case of a redundant manipulator, the governing equations, similar to those of the nonredundant manipulator, are as follows:

$$(x, y, z)^T = \boldsymbol{\Psi}(\theta_1, \ldots, \theta_m) \tag{15}$$

$$\mathbf{v} = \mathbf{J}\dot{\boldsymbol{\Theta}} = \boldsymbol{\Psi}_1\dot{\theta}_1 + \ldots + \boldsymbol{\Psi}_m\dot{\theta}_m \tag{16}$$

$$\mathbf{a} = \mathbf{J}\ddot{\boldsymbol{\Theta}} + \dot{\mathbf{J}}\dot{\boldsymbol{\Theta}} = \sum_{i=1}^{m}\boldsymbol{\Psi}_i\ddot{\Theta}_i + \sum_{i=1}^{m}\sum_{j=1}^{m}\boldsymbol{\Psi}_i\dot{\theta}_i\dot{\theta}_j \tag{17}$$

$$\boldsymbol{\Gamma} = \mathbf{M}(\boldsymbol{\Theta})\ddot{\boldsymbol{\Theta}} + \mathbf{C}(\boldsymbol{\Theta}, \dot{\boldsymbol{\Theta}}) + \mathbf{g}(\boldsymbol{\Theta}) \tag{18}$$

Combining Eqs. (17), (18), and (13), we can write the expression for end-effector acceleration as

$$\mathbf{a} = \sum_{i=1}^{m}\boldsymbol{\mu}_i\tau_i + \boldsymbol{\eta}(\boldsymbol{\Theta}, \dot{\boldsymbol{\Theta}}) \tag{19}$$

In the above equation, $\mathbf{a}$ and $\boldsymbol{\eta}$ are (3 × 1) vectors, $\boldsymbol{\eta}$ is defined in (13) and $\boldsymbol{\mu}_i$, $(i = 1, 2, \ldots m)$, is the ith column of the (3 × m) matrix $\mathbf{J}\mathbf{M}^{-1}$. At a given dynamic state $(\boldsymbol{\Theta}, \dot{\boldsymbol{\Theta}})$ of the manipulator, the vector $\boldsymbol{\eta}$ is known and Eq. (19) can therefore be considered as a mapping between the actuator torques τ_i and the end-effector acceleration $\mathbf{a}$. This mapping (19) between the joint torques and the end-effector acceleration is the basis for the dynamical resolution of redundancy proposed in this paper. As a consequence of (19), the dynamical resolution of redundancy reduces to the solution of the following problem:

Given an end-effector trajectory $\mathbf{p}(x, y, z)$ and an appropriate end-effector acceleration profile $\mathbf{a}(t)$ that yields the desired end-effector trajectory, determine the joint torques $\tau_i(t)$, $(i = 1, 2, \ldots m)$, which when applied to the manipulator will cause the (reference-point on the) end-effector to follow the desired trajectory $\mathbf{p}(x, y, z)$.

In the rest of the section, we show how the mapping (19) can be directly used to resolve redundancy without recourse to the the pseudo-inverse. Once the $\tau_i(t)$, $(i = 1, \ldots, m)$, are obtained, we will integrate the equations of motion to obtain $\boldsymbol{\Theta}(t)$, etc.

We first make the following two general observations:

(1) The resolution schemes in [15–18] attempt to solve for the joint-acceleration vector $\ddot{\boldsymbol{\Theta}}$ from the expression $\mathbf{a} = \mathbf{J}\ddot{\boldsymbol{\Theta}} + \dot{\mathbf{J}}\dot{\boldsymbol{\Theta}}$ by using an appropriate pseudo-inverse, and then use the dynamical equations of motion to solve for $\boldsymbol{\Theta}(t)$, etc.. The pseudo-inverse solution based on joint acceleration essentially minimizes $|\ddot{\boldsymbol{\Theta}}|$. We could alternatively use a pseudo-inverse scheme based on torque which would yield the torque solution $\boldsymbol{\Gamma}$; this solution would minimize $|\boldsymbol{\Gamma}|$.

(2) From the available m actuator torques τ_i, $(i = 1, 2, \ldots m)$, in the mapping (19), $(m - 3)$ actuator torques can be specified at the will of the analyst. These $(m - 3)$ "free" torques can be used, for example, to cancel the nonlinear term $\boldsymbol{\eta}(\boldsymbol{\Theta}, \dot{\boldsymbol{\Theta}})$ as discussed in the next section.

3.2 Application. One potential application for the dynamical redundancy resolution approach is the use of redundancy to cancel the nonlinearity $\boldsymbol{\eta}(\boldsymbol{\Theta}, \dot{\boldsymbol{\Theta}})$. We motivate this application by discussing the well-known method for the control of nonlinear dynamical systems known as feedback linearization [23]. For rigid robot manipulators, we can think of feedback linearization as a (nonlinear) control strategy which uses a part of each actuator torque to "cancel" the nonlinear terms in the dynamical equations. The technique is called feedback linearization for the following two reasons:

(*a*) the nonlinear terms are computed based on actual (sensed) states of the manipulator which are fedback to the controller, and

(*b*) the "new" dynamical system which results after the "cancellation" of the nonlinearities is linear or, more precisely, "feed-back linearized."

The potential advantage of feedback linearization is that one can then apply standard techniques from linear control theory to design controllers for the feedback linearized system. An alternative to feedback linearization, suggested by the mapping (19), is to make use of $(m - 3)$ "free" torques to cancel the nonlinearities. If $r = (m - 3)$ denotes the number of degrees of redundancy, then complete cancellation of the nonlinearities would require at least 3 degrees of redundancy, i.e., $r \ge 3$ in the spatial case for complete cancellation. The mapping between the actuator torques and acceleration which results after the cancellation of the nonlinearities is linear, providing the aforementioned potential advantages in control.

We now demonstrate how the actuator torques can be used to cancel the nonlinearity $\boldsymbol{\eta}(\boldsymbol{\Theta}, \dot{\boldsymbol{\Theta}})$ in the mapping (19). Assuming that the last $(m - 3)$ actuator torques are the "free" variables which will be used to cancel the nonlinearities, we set

$$\sum_{j=4}^{m}\boldsymbol{\mu}_1\tau_i + \boldsymbol{\eta} = 0. \tag{20}$$

Since $\boldsymbol{\eta}$ is a (3 × 1) vector we can arbitrarily pick three of the $(m - 3)$ "free" or "redundant" torques τ_i, $(i = 4, \ldots, m)$, as unknowns. The appropriate magnitude of these torques is

obtained by simply taking the dot product of Eq. (20) with three independent vectors in $\mathbf{R}^3$ and then simultaneously solving the three resulting scalar equations. If there are $r<3$ redundant degrees of freedom, we can only cancel nonlinearities along $r(<3)$ preferential directions.

In section 4, we use an example of a planar 3R manipulator to illustrate the application of the dynamical resolution of redundancy to the cancellation of nonlinearities.

3.3 Algorithm for Redundancy Resolution. In this subsection, we present an algorithm for the dynamical resolution of redundancy. We assume that the end-effector acceleration profile $\mathbf{a}(t)$ and the initial state $(\Theta(0), \dot{\Theta}(0))$ of the manipulator are known. The redundancy resolution scheme provides an additional set of $(m-3)$ equations in τ_i, $(i = 1,\ldots, m)$.

(i) Step 1—For the given initial state evaluate $\eta(\Theta,\dot{\Theta})$ using (13).

(ii) Step 2—Solve for $\tau_i(0)$, $(i = 1,\ldots,m)$, from the three equations in (19), the value of $\mathbf{a}$ at $t = 0$, and the $(m-3)$ equations obtained from the resolution scheme.

(iii) Step 3—Integrate the dynamical equations of motion (18) with the known initial conditions to obtain Θ, $\dot{\Theta}$, etc., at the end of the integration time-step.

(iv) Step 4—Evaluate η [Eq. (13)] at the end of the time-step.

Steps 1 through 4 are then repeated for each new time-step until the final time is reached. The time step used for the integration should be small enough that the quantities $(x'(t), y'(t), z'(t))$, $\mathbf{v}'(t)$, and $\mathbf{a}'(t)$ computed from the above procedure are very close to the given $(x(t), y(t), z(t))$, $\mathbf{v}(t)$ and $\mathbf{a}(t)$. (The coordinates $(x(t), y(t), z(t))$ of the end-effector path are either given or obtained from integration of given $\mathbf{a}(t)$).

4 Illustrative Example

In this section, we illustrate the application of the ideas developed in section 3 to a planar 3R manipulator. Both the approach based on the mapping (19) as well as the approach based on the pseudo-inverse will be applied and then compared.

4.1 The Planar 3R Manipulator. If we are only interested in the path (and therefore the position) of the end point of the 3R manipulator, then we have one degree of redundancy. The manipulator moves in a horizontal plane and therefore all terms due to gravity in the dynamical equations are identically equal to zero. Figure 1 shows a three degrees-of-freedom manipulator in the (horizontal) XY plane. There are three revolute joints, with joint variables θ_1, θ_2, and θ_3. The link lengths are a_{12}, a_{23}, and a_{34}, the masses of the links are m_i, $(i = 1, 2, 3)$, the distances to the center of gravity of the links from the joint end are r_i, $(i = 1, 2, 3)$, and the principal central moments of inertia about an axis normal to the XY plane are I_i, $(i = 1, 2, 3)$. We are interested in the motion $\mathbf{p}(x,y)$ of the end-point of link 3. The displacement equations, Ψ: $(\theta_1, \theta_2, \theta_3)$— to $(\mathbf{x},\mathbf{y})$, are

$$\mathbf{x} = a_{12}c_1 + a_{23}c_{1+2} + a_{34}c_{1+2+3},$$

$$\mathbf{y} = a_{12}s_1 + a_{23}s_{1+2} + a_{34}s_{1+2+3}, \tag{21}$$

where c_1, s_1, c_{1+2}, s_{1+2}, etc., represent, respectively, $\cos(\theta_1)$, $\sin(\theta_1)$, $\cos(\theta_1+\theta_2)$, $\sin(\theta_1+\theta_2)$, etc.

The velocity and acceleration are given by

$$\mathbf{v} = \Psi_1\dot{\theta}_1 + \Psi_2\dot{\theta}_2 + \Psi_3\dot{\theta}_3,$$

$$\mathbf{a} = \sum_{i=1}^{3}\Psi_i\ddot{\theta}_i + \sum_{j=1}^{3}\sum_{i=1}^{3}\Psi_{ij}\dot{\theta}_i\dot{\theta}_j, \tag{22}$$

where Ψ_i and Ψ_{ij} are the first and second derivatives (with respect to the θ_i's) of the mapping function Ψ given by (21), and $\dot{\theta}_i$ and $\ddot{\theta}_i$ are the time derivatives of θ_i. Detailed expressions

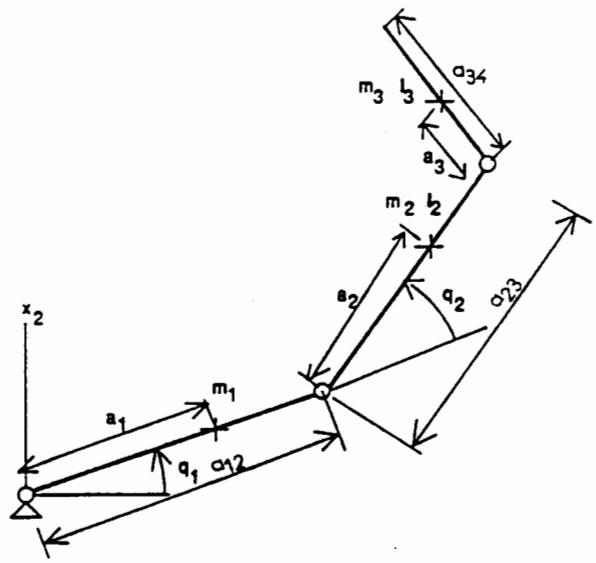

Fig. 1 A planar 3R manipulator

for Ψ_i and Ψ_{ij}, $(i = 1, 2, 3)$, $(j = 1, 2, 3)$, are given in Appendix A.

The equations of motion are

$$\Gamma = \mathbf{M}\ddot{\Theta} + \mathbf{C}(\Theta, \dot{\Theta}), \tag{23}$$

and we can express the end-effector acceleration as

$$\mathbf{a} = \mu_1\tau_1 + \mu_2\tau_2 + \mu_3\tau_3 + \eta \tag{24}$$

In the above equation,

$$\mu_1 = \Psi_1 m'_{11} + \Psi_2 m'_{12} + \Psi_3 m'_{13},$$

$$\mu_2 = \Psi_1 m'_{12} + \Psi_2 m'_{22} + \Psi_3 m'_{23},$$

$$\mu_3 = \Psi_1 m'_{13} + \Psi_2 m'_{23} + \Psi_3 m'_{33}, \tag{25}$$

$$\eta = \sum_{j=1}^{3}\sum_{i=1}^{3}\Psi_{ij}\theta\theta_j - \sum_{i=1}^{3}\mu_i C_i, \tag{26}$$

where m'_{ij}, $(i, j = 1, 2, 3)$, are the elements of the inverse of the mass matrix, and C_i, $(i = 1, 2, 3)$, are the elements of $\mathbf{C}(\Theta, \dot{\Theta})$. Detailed expressions for the m'_{ij}, $(i = 1, 2, 3)$, $(j = 1, 2, 3)$, and C_i, $(i = 1, 2, 3)$, are given in the Appendix.

The numerical values of the geometric and the inertia parameters are as follows:

$I_1 = 0.0644\text{kgm}^2$, $I_2 = 0.0161\text{kgm}^2$, $I_3 = 0.004\text{kgm}^2$

$m_1 = 2.254\text{kg}$, $m_2 = 2.177\text{kg}$, $m_3 = 1.0531\text{kg}$

$r_1 = 0.1960\text{m}$, $r_2 = 0.0980\text{m}$, $r_3 = 0.0490\text{m}$

$a_{12} = 0.3048\text{m}$, $a_{23} = 0.1524\text{m}$, $a_{34} = 0.0762\text{m}$

4.2 Simulation Results. For the purposes of simulation and of illustrating the proposed dynamical resolution schemes, the end-point of the third link was commanded to follow a circular path centered at (0.141, 0.116) with radius 0.0222m. The initial values of $(\theta_1, \theta_2, \theta_3)$ are (0, 135, 45) degrees. The initial values of $\dot{\theta}_i$, $(i = 1, 2, 3)$, were chosen to be zero. The initial (x, y) coordinates of the tip of the manipulator (obtained from the kinematic Eqs. (21)) are (0.1208, 0.1078). A smooth acceleration profile $\mathbf{a}(t)$ was chosen so that the end-point of the third link of the manipulator completes the circle in 1.0 sec. The desired trajectory and acceleration profile are shown in Fig. 2 and Fig. 3, respectively.

We experimented with three resolution strategies. The first was a very simple strategy of setting one of the torques to zero.

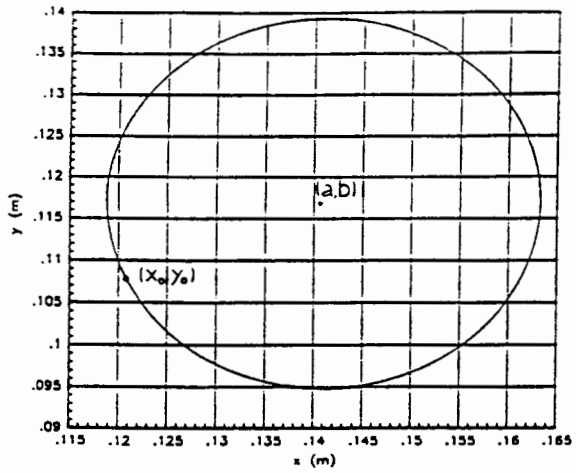

Fig. 2 Input trajectory of the tip of the end-effector

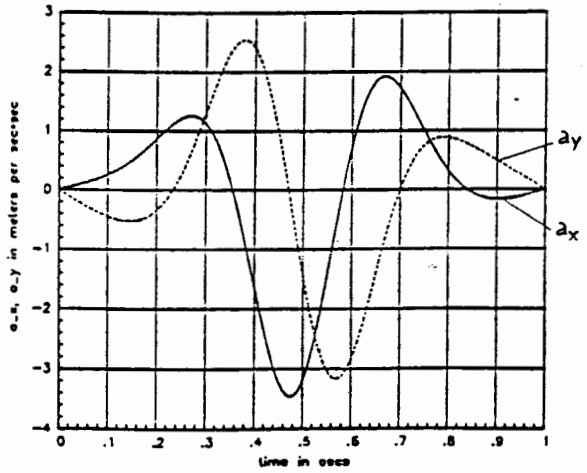

Fig. 3 Input acceleration profile

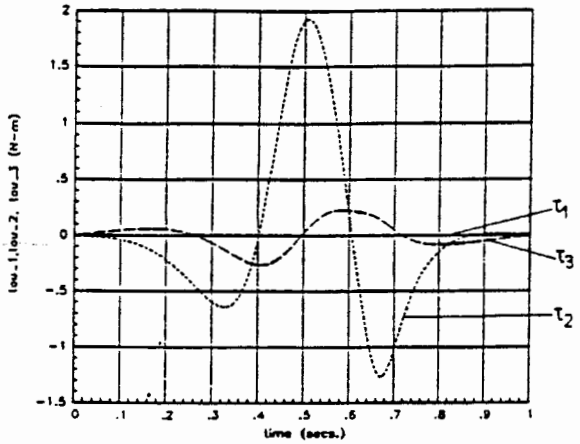

Fig. 4 Case 1-torque profiles for $\tau_1 = 0$

We chose to set $\tau_1 = 0.0$ as typically the first actuator experiences the maximum torque. The second strategy was the application of the pseudo-inverse method to the mapping (19) in order to obtain the torques at the three joints. The third strategy was partial cancellation of η—since there is only one redundant degree of freedom, we can cancel η in only one direction. We chose to cancel η in the direction of μ_3.

The aims of the simulations are to illustrate the theory developed in Section 3 and to obtain some insight into the various redundancy resolution schemes by comparing the torque profile obtained in each case.

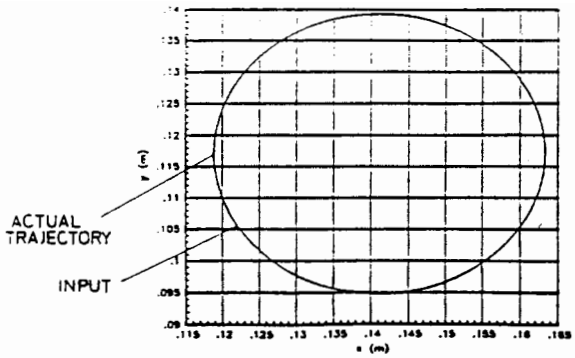

Fig. 5 Comparison of input and actual trajectory for Case 1

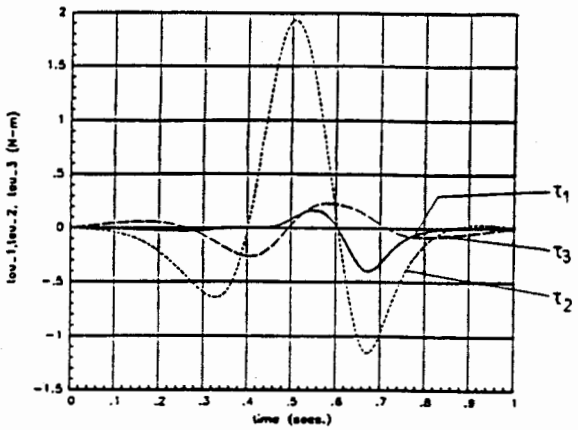

Fig. 6 Case 2-torque profiles for the pseudo-inverse solution

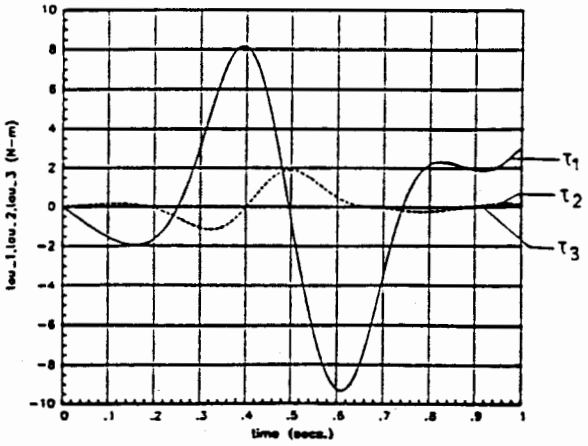

Fig. 7 Case 3-torque profiles for partial cancellation of $\eta(\Theta, \dot{\Theta})$

In all cases the integration was performed by a variable step Kutta-Merson predictor-corrector method.

Case 1—$\tau_1 = 0$

Figure 4 shows the torque profiles for $\tau_1 = 0$. It can be seen that the maximum torque is required from actuator 2. The maximum value of τ_2 is approximately 1.9N-m at $t = 0.5$ seconds. In Fig. 5, the trajectory of the tip of the end-point of the third link is compared with the desired trajectory. The error is very small and is due to build-up of errors during integration. The strategy of setting the base actuator torque $\tau_1 = 0$ is useful for manipulators operating in microgravity environments [24], where an important requirement is that no torque (and force) be transmitted to the base of the manipulator (i.e., τ_1 must be equal to zero).

Case 2—The Pseudo-inverse solution.

The torque profiles are shown in Fig. 6. They are very similar to the ones obtained in Case 1. As in Case 1 the maximum

torque is required from the actuator at the second joint. The trajectory of the tip (not shown) again follows the desired trajectory very closely with insignificantly small errors building up towards the end.

Case 3—Partial cancellation of $\eta(\Theta, \dot{\Theta})$

The torque profiles are shown in Fig. 7. In this case the torque required from the actuator at the first joint (τ_1) is significantly larger than the other actuator torques. The torques required from actuators at joints 2 and 3 are comparable to the previous two cases. The trajectory of the end-point again very closely followed the desired trajectory with negligibly small errors building up towards the end.

5 Discussion

The trajectory chosen in our example was a circle. The method also works for straight line or piece-wise straight line trajectories. Care must however be taken if there are singularities in the trajectory. It was observed during simulations that if there are singularities in the trajectories (θ_2 or θ_3 equal to 0 or 180 degrees for the current example), one cannot partially cancel the nonlinear term. This is due to the fact that the torques at the joints become very large as the end-effector approaches a singularity. The ability to achieve the desired performance measures will also be limited by the maximum and minimum torques available at the actuators. In the present example, the simulations have not taken into account the limits on the actuator torques. The magnitudes of joint torques obtained from the dynamic resolution of redundancy clearly depend on which actuator torques are chosen as the "free" joint torques.

We have dealt only with the positional aspects of the motion of the rigid body. To account for the rotational motion of the rigid body, we need to develop the map between joint torques and angular acceleration of the end-effector.

In conclusion, in this paper we have presented an alternative approach for the dynamic resolution of redundancy. This approach does not require the use of the pseudo-inverse of the Jacobian or any other matrix. As an application of our approach, we have shown how the nonlinear terms in the equations of motion can be cancelled by use of redundancy. Finally, we have illustrated the new approach with an example of a planar 3R manipulator.

6 Acknowledgments

The authors would like to acknowledge the use of computer facilities at Integrated Systems Inc. The research was partially supported by the Engineering Design Research Center of Carnegie Mellon University.

References

1 Paul, R. P., and Stevenson, C. N., 1983, "Kinematics of Robot Wrists," *Int. Journal of Robotics Research*, Vol. 2, No. 1, pp. 31-38.

2 Yoshikawa, T., 1985, "Manipulability and Redundancy Control of Robotic Mechanisms," *IEEE Conference on Robotics and Automation*, pp. 1004-1009, March 25-28, St. Louis.

3 Takase, K., Inoue, H., and Sato, K., 1974, "The Design of an Articulated Manipulator with Torque Control Ability," *Proc. 4th Int. Symp. Industrial Robots*, pp. 261-270, Nov. 19-21.

4 Yoshikawa, T., 1984, "Analysis and Control of Robotic Manipulators with Redundancy," *Robotics Research: The First International Symposium*, MIT Press, pp. 735-748.

5 Trevelyan, J. P., Kovesi, P. D., and Ong, M. C. H., 1984, "Motion Control for a Sheep Shearing Robot," *Robotics Research: The First International Symposium*, MIT Press, pp. 175-190.

6 Liegeois, A., 1977, "Automatic Supervisory Control of Configuration and Behavior of Multibody Mechanisms," *IEEE Trans. Systems, Man, Cybernetics*, SMC-7, pp. 868-871.

7 Baillieul, J., Hollerbach, J. M., and Brockett, R., 1984, "Programming and Control of Kinematically Redundant Manipulators," *Proc. 23rd IEEE Conference on Decision and Control*, Dec. 12-14, Las Vegas, pp. 768-774.

8 Klein, C. A., 1985, "Use of Redundancy in Design of Robotic Systems," *Robotics Research: The Second International Symposium*, MIT Press, pp. 206-214.

9 Hanafusa, H., Yoshikawa, T., and Nakamura, Y., 1981, "Analysis and Control of Articulated Robot Arms with Redundancy," *Prep. 8th IFAC World Congress*, pp. XIV-78-83.

10 Nakamura, Y., and Hanafusa, H., 1985, "Task Priority Based Redundancy Control of Robot Manipulators," *Robotics Research: The Second International Symposium*, MIT Press, pp. 155-162.

12 Vukobratovic, M., and Kicanski, M., 1984, "A Dynamic Approach to Nominal Trajectory Synthesis for Redundant Manipulators," *IEEE Trans. Systems, Man, and Cybernetics*, Vol. 1, No. 4.

13 Fournier, A., and Khalil, W., 1977, "Coordination and Reconfiguration of Mechanical Redundant Systems," *Proc. Int. Conf. on Cybernetics and Society*, Washington D.C., pp. 227-231.

14 Chang, P. H., 1986, "A Closed-Form Solution for Control of Manipulators with Kinematic Redundancy," *Proc. IEEE Int. Conf. Robotics and Automation*, San Francisco, April, pp. 9-14.

15 Khatib, O., 1986, "Redundant Manipulators and Kinematic Singularities: The Operational Space Approach," *Sixth CISM-IFToMM Symposium on Theory and Practice of Robots and Manipulators*, Sept. 9-12, Cracow, Poland.

16 Khatib, O., 1983, "Dynamic Control of Manipulators in Operational Space," *6th IFToMM Congress on Theory of Machines and Mechanisms*, New Delhi, Dec., pp. 1128-1131.

17 Hollerbach, J. M., and Suh, Ki. C., 1985, "Redundancy Resolution of Manipulators through Torque Optimization," *IEEE Conference on Robotics and Automation*, pp. 1016-1021, March 25-28, St. Louis.

18 Hollerbach, J. M., and Suh, Ki. C., 1987, "Local versus Global Torque Optimization of Redundant Manipulators," *IEEE Conference on Robotics and Automation*, Raleigh, North Carolina, pp. 619-624.

19 Ghosal, A., 1986, "Instantaneous Properties of Multi-degree-of-freedom Motions," Ph.D. Thesis, Stanford University, Dept. of Mechanical Eng., July 1986.

20 Ghosal, A., and Roth, B, 1988, "A New Approach for Kinematic Resolution of Redundancy," *Int. Journal of Robotics Research*, Vol. 7, No. 2, pp. 22-35.

21 Rao, C. R., and Mitra, S. K., 1971, "Generalized Inverse of Matrices and its Application," John Wiley & Sons.

22 Desa, S., and Kim, Y. Y., "Analysis of the Maps of Actuator Torques and Joint-Velocities to End-effector Acceleration for Planar Manipulators," ASME JOURNAL OF MECHANICAL DESIGN, to appear.

23 Spong, M. W., and Vidyasagar, M., 1989, "Robot Dynamics and Control," John Wiley and Sons.

24 Chung, C. L., and Desa, S., 1989, "A Global Approach for Using Kinematic Redundancy to Minimize Base Reactions of Manipulators," *15th ASME Design Automation Conference, Montreal, Canada, Sept. 17-20, 1989, Advances in Design Automation-1989*, Vol. 3, pp. 297-303, ASME.

APPENDIX

In this appendix the detailed expressions for Ψ_i, Ψ_{ij}, $(i, j = 1, 2, 3)$, the components of the inverse mass matrix, m'_{ij}, $(i, j = 1, 2, 3)$, and the components of $\mathbf{C}(\Theta, \dot{\Theta})$ are given. In Eqs. (A1)-(A4) below, a_{ij}, I_i, m_i, r_i are the quantities defined in section 4.1.

The expressions for Ψ_i and Ψ_{ij}, $i, j = 1, 2, 3$, are as follows;

$$\Psi_1 = a_{12}(-s_1, c_1)^T + a_{23}(-s_{1+2}, c_{1+2})^T + a_{23}(-s_{1+2+3}, c_{1+2+3})^T$$

$$\Psi_2 = a_{23}(-s_{1+2}, c_{1+2})^T + a_{34}(-s_{1+2+3}, c_{1+2+3})^T$$

$$\Psi_3 = a_{34}(-s_{1+2+3}, c_{1+2+3})^T$$

$$\Psi_{11} = -a_{12}(c_1, s_1)^T - a_{23}(c_{1+2}, s_{2+3})^T + -a_{23}(-s_{1+2+3}, c_{1+2+3})^T$$

$$\Psi_{22} = -a_{23}(c_{1+2}, s_{2+3})^T - a_{23}(-s_{1+2+3}, c_{1+2+3})^T$$

$$\Psi_{33} = -a_{23}(-s_{1+2+3}, c_{1+2+3})^T$$

$$\Psi_{12} = \Psi_{22}$$

$$\Psi_{13} = \Psi_{33}$$

$$\Psi_{23} = \Psi_{33} \tag{A1}$$

The expressions for m'_{ij}, $(i = 1, 2, 3)$, $(j = 1, 2, 3)$, are as follows: